Scheduling of Collaborative Sequential Compressed Sensing Over Wide Spectrum Band

Jie Zhao, *Student Member, IEEE,* Qiang Liu, *Member, IEEE,* Xin Wang, *Member, IEEE,* and Shiwen Mao, *Senior Member, IEEE*

***Abstract*—The cognitive radio (CR) technology holds promise to significantly increase spectrum availability and wireless network capacity. With more spectrum bands opened up for CR use, it is critical yet challenging to perform efficient wideband sensing. We propose an integrated sequential wideband sensing scheduling framework that concurrently exploits sequential detection and compressed sensing (CS) techniques for more accurate and lower-cost spectrum sensing. First, to ensure more timely detection without incurring high overhead involved in periodic recovery of CS signals, we propose smart scheduling of a CS-based sequential wideband detection scheme to effectively detect the PU activities in the wideband of interest. Second, to further help users under severe channel conditions identify the occupied sub-channels, we develop two collaborative strategies, namely, joint reconstruction of the signals among neighboring users and wideband sensing-map fusion. Third, to achieve robust wideband sensing, we propose the use of anomaly detection in our framework. Extensive simulations demonstrate that our approach outperforms peer schemes significantly in terms of sensing delay, accuracy and overhead.**

***Index Terms*—cognitive radio; sequential detection; wideband sensing; compressed sensing; cooperative sensing.**

I. Introduction

The ubiquity of wireless-enabled computing and communications devices has led to ever increasing demands on network capacity to support a variety of rich and resource-consuming wireless applications. As a promising technology, cognitive radio (CR) has attracted significant interests and efforts from academia and industry [35], where CR devices have been applied to intelligently and dynamically identify and aggregate spectrum holes to increase network capacity [13]. A core function of a CR, or secondary user (SU), is to sense the spectrum and detect the presence/absence of ambient primary users (PUs). Many studies have been conducted to improve the effectiveness of spectrum sensing, although most apply only to narrowband scenarios. Wideband spectrum sensing has become increasingly important for CRs to obtain a "wider" view of the spectrum: It enables a CR to find spectrum resources more flexibly and quickly, and also allows a CR-enabled network to transmit data at a higher rate with more available spectrum resources.

Despite its great potential, wideband sensing is still a challenging task. A wideband can be generally divided into sub-bands or sub-channels, whose occupancy status (i.e., whether occupied by PUs) can be determined via sensing. It is possible to sense all the narrow sub-channels one by one with a proper channel sensing order [32], which is applicable for a narrowband; however, for a wideband with an extremely large number of sub-channels, sensing each channel would incur large overhead and delay. Alternatively, CRs can sense the wideband directly with high-end components, e.g., wideband antenna and radio frequency (RF) front-end, and high-speed analog-to-digital converter (ADC). To avoid the use of these expensive components, compressed sensing (CS) [6], [10] has been exploited to reduce the total number of samples required [2], [26]. An application running over a long duration cannot simply sense a channel once, but rather should sense it periodically to avoid interfering with returning legacy users. Due to the higher computational complexity for CS recovery in wideband sensing, it would be very expensive to directly apply CS methods for periodic sensing. Spectrum sensing becomes even harder when a user receives weak signals due to fluctuating environmental dynamics such as channel fading. Although cooperative sensing may help overcome this problem, simply applying cooperative wideband sensing using samples from a large number of users would involve very high signaling overhead and computational complexity.

In this work, we consider a CR network with multiple users and propose a *cooperative sequential compressive sensing* framework which incorporates sensing scheduling into two major steps: *wideband signal occupancy detection* to detect PU presence in a wideband of interest, and *cooperative wideband compressive sensing* to determine which sub-bands are actually occupied in the wideband. The first step applies smart scheduling of both sequential and compressed sensing to detect if there exist PU signals in a wideband without the need for frequent and complex signal reconstruction. In contrast to conventional cooperative spectrum sensing, which directly exploits collaboration among users without considering the information exchange overhead, the second step is developed into two cooperative schemes: (1) joint reconstruction of signals from multiple SUs to improve sensing

Manuscript received March 25, 2017; revised September 8, 2017 and December 10, 2017; accepted December 11, 2017; approved by IEEE/ACM TRANSACTIONS ON NETWORKING Editor J. Huang. Date of publication January 17, 2018; date of current version February 14, 2018. *(Corresponding author: Jie Zhao.)*

J. Zhao and X. Wang are with the Department of Electrical and Computer Engineering, Stony Brook University, Stony Brook, NY 11794 USA (e-mail: jie.zhao@stonybrook.edu; x.wang@stonybrook.edu).

Q. Liu is with the Oak Ridge National Laboratory, Computational Sciences and Engineering Division, Oak Ridge, TN 37831 USA (e-mail: liuq1@ornl.gov).

S. Mao is with the Department of Electrical and Computer Engineering, Auburn University, Auburn, AL 36849, USA (e-mail: smao@ieee.org).

Digital Object Identifier 10.1109/TNET.2017.2787647

This work is supported by NSF ECCS 1408247, NSF ECCS 1731238, ONR N00014-13-1-0209 and AFOSR FA9550-14-1-0193.

accuracy, thereby reducing the number of samples required for exchange, and (2) wideband status map fusion among multiple users with low-cost signaling overhead.

To further improve the accuracy of wideband sensing, we propose the use of anomaly detection in our framework. Spectrum sensing can fail in environments with significant amounts of anomalous data. Unlike a regular channel state change due to the arrival/departure of the PU, the anomalies (i.e., data outliers) could originate from various sources, such as unusual environmental events (thunderstorms, electric spark, etc.), internal hardware miscalibration that results in erroneous measurements, and malicious attacks from other nodes. In the presence of abnormal readings, measurements obtained at the affected nodes are contaminated. The anomalies need to be accurately identified to ensure robust spectrum sensing and protect against attacks. Furthermore, it is also vitally important to evaluate if a node is functioning normally based on the quantity of abnormal readings so that a network manager can take further actions if necessary.

The major contributions of our work are as follows:

- We propose scheduling of compressed-sensing-based sequential wideband detection, leveraging both CS and sequential detection techniques for accurate and low-overhead PU detection. Specifically, we perform sequential detection based on sub-Nyquist samples directly, without incurring high CS recovery overhead, and adapt the scheduling of sequential detection to improve the detection performance.
- We exploit both intra-signal temporal correlation and inter-signal spatial correlation to schedule more efficient cooperative compressed spectrum sensing by proposing two cooperative schemes: (a) joint reconstruction of the signals among neighboring users to reduce the number of samples required to achieve a given spectrum recovery quality measure, thus reducing the number of samples sent from each user and the resulting communication overhead, and (b) wideband status map fusion that only incurs limited information exchange among the users.
- We propose an anomaly detection method to enable robust data transmission/reception and more accurate wideband sensing.
- We perform extensive simulations to validate and demonstrate the major advantages of our design.

The rest of this paper is organized as follows. Section II provides an overview of related work. We introduce our system framework and sensing infrastructure in Section III, and describe our sequential wideband detection with compressive sampling in Section IV. Cooperative wideband compressive sensing and anomaly detection are presented in Section V. In Section VI, we provide extensive simulation results with detailed discussions. The paper is concluded in Section VII.

II. Related Work

The majority of studies on spectrum sensing focus on detection quality for one-time sensing. However, the presence of uncertainty, such as noise, interference, channel fading, and anomalies, makes it a daunting task to yield accurate one-time detection decisions. Moreover, many applications run over a long duration, and one time sensing is simply inadequate. Recent efforts have attempted to detect the status of narrowband channels based on a sequence of sensing data. Specifically, sequential analysis [28] has been carried out in [12], [14], [21] for spectrum sensing to obtain a better performance such as a smaller latency and more accurate decisions. Different from existing efforts, the focus of this paper is on effective detection of activities of the legacy wireless systems over a wide spectrum. Sequential detection is applied over sparse samples of signals (rather than Nyquist samples) to facilitate low-cost coarse signal monitoring before determining the actual sub-channels occupied by the primary signals. Besides applying sequential spectrum sensing, a fundamental difference between our work and related studies such as [12], [14], [21] is our focus on sensing scheduling that is adapted over time to speed up the decision without introducing a high overhead.

Compressed sensing (CS) is a useful tool for wideband spectrum sensing and analysis. Following the principle of CS, if a signal is sparse in certain domain, it can be recovered from far fewer samples than required by the Shannon-Nyquist sampling theorem. In a wide spectrum band, normally only some parts of the spectrum are occupied. CS can be exploited to reduce the high sampling rate requirement of the wide-band signal through sub-Nyquist sampling and then fully reconstruct the signal. Tian *et al.* [26] aim to identify wideband spectrum holes with sub-Nyquist samples used along with a wavelet-based edge detector. Similarly, in [2], [3], [27], [29], various wideband spectrum sensing schemes based on CS are proposed. The flexible channel division scheme with CS is proposed in [23], and efforts are made in [24] to reduce the computational complexity of CS with information pulled from a geo-location database. Romero *et al.* in [25] propose to exploit the second-order statistics such as the covariance to improve the CS performance. Although these methods show that it is promising to apply CS to wideband sensing, the complexity involved in CS signal reconstruction makes it difficult to use for long-term spectrum monitoring desired by practical cognitive radio systems. We propose to concurrently exploit sequential detection and compressed sensing for accurate and lightweight wideband sensing. Although the scheduling of periodic sequential sensing has been shown to improve the spectrum sensing performance [16], [17], it would be very expensive to perform CS periodically. Our framework is not dependent on any particular wideband sampling method, and the aforementioned wideband CS schemes can be applied in our algorithm whenever there is a need to detect detailed spectrum occupancy conditions in a wideband.

The performance of detection is often compromised by environmental dynamics such as noise uncertainty, fading, and shadowing. To mitigate impacts of those issues, cooperative sensing [1], [4], [9], [15], [18] has been proposed in the literature and is shown to be effective in improving the detection performance by exploiting spatial diversity among users. However, conventional cooperative schemes are for narrow-band sensing without much information exchange. There are also efforts on cooperative wideband sensing based

on CS. In [30], [31], distributed compressed wideband sensing schemes are proposed. Sun *et al.* in [2] propose a multi-slot CS-based wideband sensing algorithm where sensing is terminated once the currently recovered spectrum is deemed satisfactory. Different from existing works, our cooperative wideband sensing is performed after a wideband has been detected with PU signals. Taking into account the bandwidth consumption of information exchange, we study two cooperative schemes for wideband sensing: one exploiting joint reconstruction of multiple signals with the aim of reducing the CS reconstruction overhead and the other employing collaborative fusion with limited information exchange.

In order to improve the detection performance and reduce the computational overhead, Ma *et al.* in [20] exploit the joint sparse properties of wideband signals among multiple SUs. Rather than following the joint sparsity model (JSM) type two (JSM-2) [11] to consider the common sparse support of cooperative users assuming all users detect the same spectrum occupancy conditions, our scheme exploits JSM type one (JSM-1) [5] to consider common sparse components while also taking into account the difference in spectrum sensed by individual users. In addition, we consider many other design factors in cooperative sequential compressed sensing over wideband, such as scheduling of sequential detection, fusion of spectrum maps and anomaly detection.

We have introduced CS-based cooperative sequential wideband sensing in our earlier paper [34]. In this work, we provide more detailed analyses and theoretical proofs on certain properties of our scheme. In addition, we propose a set of new schemes to enhance our previous design, including additional sampling after detection decision, two new wideband sensing map fusion schemes and an anomaly detection methodology. These additional components help to further improve the sequential detection efficiency and wideband spectrum map reconstruction accuracy. Finally, we have performed more extensive performance evaluations and analyses to demonstrate the effectiveness of our proposed strategies.

The goal of this work is to enable efficient cooperative wideband sensing. Different from the literature work, to reduce the sensing overhead and improve the sensing performance, our scheme is composed of two major steps: (a) following the principles of sequential detection and CS, we adaptively schedule CS-based sequential detection (without CS reconstruction) to detect PU presence in the wideband efficiently in a timely manner; (b) to enhance the detection performance with cooperative sensing, we further take advantage of correlation (joint sparse property) among users to develop two collaborative schemes to more effectively obtain the detailed wideband occupance status from the signals sensed in the sequential detection. Furthermore, anomaly detection is incorporated into our framework to alleviate the impacts of abnormal readings in data and improve the overall wideband sensing performance. Real-world wireless applications are prone to data anomalies/outliers, and we utilize combined sparsity to simultaneously capture both the signals of interest and anomalies based on the theory of overcomplete representation basis [19].

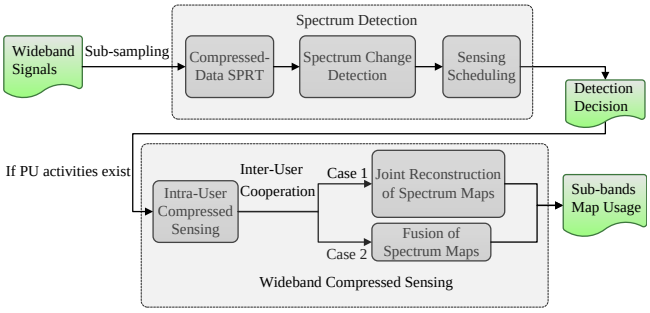

Figure 1: Framework overview

III. System Framework and Sensing Infrastructure

We consider a general CR network with a set of CR nodes, each capable of sensing the wide spectrum band in order to find unoccupied channels for secondary data transmission. PUs generally alternate between periods of being active and idle, and it is critical for CRs to detect the changes in the channel occupancy state. Once PU activities are detected, CRs also need to efficiently reconstruct the spectrum usage map within the wideband to identify the spectrum available in finer detail. In this section, we introduce first our cooperative wideband detection and sensing framework, and then the infrastructure for wideband compressed sensing and periodic sensing.

A. Framework Overview

In order to detect PU existence and reappearance in a timely fashion, each user periodically senses the wide spectrum band. As CS recovery involves high computational complexity, reconstructing the signals in each sensing period could be costly. Instead, we propose a framework with the wideband sensing carried out in two major stages, as shown in Figure 1: (1) detection of PU activities within the wideband (Section IV), and (2) cooperative wideband sensing of sub-band availability (Section V).

In the first stage, each SU first sub-samples the wideband spectrum in each sensing period, and then performs the Sequential Probability Ratio Test (SPRT) based on sub-sampled data (Section IV-A). If the data gathered for SPRT suggest that there might be spectrum status change underway, it will trigger the further setup of the sensing schedule (Section IV-C). After the wideband spectrum is detected to have active PUs, CS recovery is further invoked to identify the occupancy status of sub-channels in the wideband. As a prerequisite for cooperative CS, we will first study the intra-user compressed sensing (Section V-A). During either stage, if a user receives very weak signals as a result of severe channel fading, it would be hard for the user to correctly make a decision. The user can then request collaboration from its neighbors on demand. Before the data exchange, anomaly detection (Section V-D) can be implemented by each user to improve the accuracy of data to be used in cooperation. We propose two major collaboration methods: neighboring nodes collaborate in performing joint CS reconstruction of the spectrum map (Section V-B) or fusing spectrum maps

(Section V-C) to identify the sub-channels occupied at a lower signaling cost.

B. Wideband Compressed Sensing

A wideband can usually be divided into sub-bands/sub-channels. In Figure 2, a wide spectrum band ranging from 0 to W(Hz) is equally divided into J sub-bands, each with bandwidth W/J (Hz). For example, for a 0∼1 GHz wideband with each sub-channel occupying 1 kHz, the number of sub-channels is 10^6. Within a wideband of interest, depending on the PU activities, each sub-band can have different and time-varying occupancy states. One way to learn the usage conditions of a wide spectrum band is to directly apply the traditional narrowband detection methods to sense the sub-bands one by one [32]. For a wideband with a fairly large number of sub-channels, however, this may bring unacceptable overhead and sensing delay. Another way is to equip CRs with components such as wideband antenna, wideband RF front-end, and high-speed ADC to perform sensing over the wideband directly. For wideband sensing, a major challenge is that the required Nyquist sampling rate can be excessively high. For example, a 0∼500 MHz wideband requires a Nyquist sampling rate of 1 GHz, which would incur high ADC element costs and processing overhead. This motivates us to explore the use of CS to reduce the required sampling rate significantly for wideband sensing.

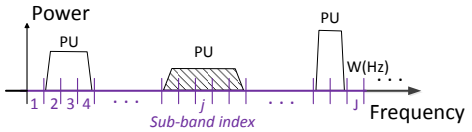

Figure 2: Frequency division for wideband CRs

The CS theory suggests that if an N-dimensional signal is sparse in a certain domain, one can fully recover the signal by using only $\Omega(\log N)$ linear measurements; in other words, CS takes advantage of the sparsity within the signal to significantly reduce the sampling rate. As a wideband is often sparsely occupied by PUs as shown in Figure 2, CS can be applied for wideband sensing. For a wideband of bandwidth W, after obtaining the spectrum occupancy conditions, a CR can transmit data over the spectrum holes.

To detect the spectrum usage condition, a CR can take samples of the received signal $d_{\mathrm{c}}(t)$ for a duration of T_s, where the received signal is composed of PU signals and background noise. By using a certain sampling rate f_N over the sensing time T_s, we can obtain a discrete-time sequence $d[n] = d_{\mathrm{c}}(\frac{n}{f_N}),\ n = 0, 1, \cdots, N-1$, in a vector form $\mathbf{d} \in \mathbb{C}^{N\times 1}$. Here, $N = T_s f_N$ is usually chosen to be a positive integer. Based on the Nyquist sampling theory, the sampling rate is required to exceed $2W$, i.e., $f_N > 2W$.

To reduce the need for high frequency sampling at the RF front end, in our CS framework, an SU's detector collects the ambient signal at a certain sub-Nyquist sampling rate f_{sub} smaller than the Nyquist rate f_{nyq}. An $M \times N$ ($M < N$) measurement matrix $\mathbf{\Phi}$ is applied to perform sub-sampling, where M and N denote the number of sub-Nyquist and Nyquist samples, respectively. If the sensing duration within a period T_p is T_s, then $M = f_{sub}T_s$ and $N = f_{nyq}T_s$.

If there is any PU signal within the wideband of interest, the sub-sample vector will be expressed as

$$\mathbf{y} = \mathbf{\Phi}(\mathbf{d} + \mathbf{n}') = \mathbf{\Phi}\mathbf{d} + \mathbf{n} = \mathbf{\Phi}\mathbf{\Psi}\mathbf{x} + \mathbf{n} = \mathbf{A}\mathbf{x} + \mathbf{n}, \quad (1)$$

where the sub-Nyquist measurements are $\mathbf{y} \in \mathbb{R}^{M\times 1}$, the sparse vector in Fourier spectrum domain $\mathbf{x} \in \mathbb{R}^{N\times 1}$, the additive noise in the wideband $\mathbf{n}'$, the sampled noise $\mathbf{n} \in \mathbb{R}^{M\times 1}$, and the sensing matrix $\mathbf{A} \in \mathbb{R}^{M\times N}$.

Given the measurements $\mathbf{y}$, the unknown sparse vector $\mathbf{x}$ can be reconstructed by solving the following convex optimization problem:

$$\min \quad \|\mathbf{x}\|_{\ell_1} \quad (2a)$$

$$\text{s.t.} \quad \|\mathbf{\Phi}\mathbf{d} - \mathbf{y}\|_{\ell_2} \le \epsilon \quad (2b)$$

$$\mathbf{d} = \mathbf{\Psi}\mathbf{x} \quad (2c)$$

where the parameter ϵ is the bound of the error caused by noise $\mathbf{n}$, and ℓ_p denotes the ℓ_p-norm ($p = 1, 2, ...$). The solution can be equivalently expressed as

$$\hat{\mathbf{x}} = \underset{\mathbf{u}:\ \|\mathbf{y}-\mathbf{A}\mathbf{u}\|_{\ell_2}\le\epsilon}{\arg\min} \|\mathbf{u}\|_{\ell_1}. \quad (3)$$

The signal $\mathbf{d} = \mathbf{\Psi}\mathbf{x}$ can then be recovered as $\hat{\mathbf{d}} = \mathbf{\Psi}\hat{\mathbf{x}}$. In addition to this convex optimization approach (ℓ_1 minimization [7]), there also exist several iterative/greedy algorithms such as Cosamp [22]. Such convex or greedy approaches are generally called reconstruction algorithms.

Charbiwala *et al.* [8] show that if the signal spectrum vector $\mathbf{x} = \mathbf{\Psi}^{-1}\mathbf{d}$ is sparse, then $\mathbf{\Phi} = \mathbf{A}\mathbf{\Psi}$ is essentially an $M \times N$ random sampling matrix constructed by selecting M rows independently and uniformly from an $N \times N$ identity matrix $\mathbf{I}$. This measurement matrix $\mathbf{\Phi}$ can be trivially implemented by pseudo-randomly sub-sampling the original signal $\mathbf{d}$. As we can adopt the inverse Discrete Fourier Transform (DFT) matrix as the sparse dictionary $\mathbf{\Psi}$, the measurement matrix will be reflected by sub-Nyquist sampling. For a time domain signal with length N, this sub-Nyquist measurement corresponds to a smaller $M < N$ number of samples. If the spectral sparsity level K of $\mathbf{x}$ is known, one can choose the number of measurements M to ensure the quality of spectral recovery.

C. Periodic Sensing Structure

Figure 3 illustrates the periodic channel sensing structure, where the channel detection time (CDT) is the maximum allowed time to make a sensing decision. A CDT usually consists of multiple sensing-transmission periods, each called a *sensing period* T_p. In this work, as in the 802.22 WRAN standard, the *sensing time* T_s is fixed, e.g., 1 ms, and T_p may only take values that are multiples of a MAC frame size (FS), e.g., 10 ms due to many higher-layer concerns such as synchronization. The *detection overhead* (R_{do}) describes the proportion of time dedicated to the PU detection task and is defined as the ratio between T_s and T_p, i.e., $R_{do} = T_s/T_p$. Scheduling of sequential detection will have a significant influence on the detection overhead as will be shown later.

Figure 3: Channel detection time CDT, sensing period T_p, and sensing time T_s

IV. Spectrum Detection based on Sequential Compressed Sensing

In order to reduce the overall spectrum sensing overhead, as shown in our framework in Figure 1, we divide our sensing process into two major stages: 1) cooperatively detecting if there exist PUs in a wide spectrum band, and 2) estimating the detailed spectrum usage conditions within the wideband detected with PUs by constructing a spectrum occupancy map. In this section, we describe the first stage, in which each SU periodically sub-samples the wideband and detects the spectrum activities via group-based compressive sequential detection. If a user receives very weak signals as a result of severe channel conditions such as fading, it can send a request to its neighbors, and perform collaborative sequential detection based on responses from the neighboring users. We analyze the condition for stopping the data collection and making a detection decision in Section IV-B, and introduce additional procedures that can be taken to speed up the decision making in Section IV-C.

A. Cooperative Grouped-Compressed-Data SPRT

The classical sequential detection method, Wald's Sequential Probability Ratio Test (SPRT) [28], inputs each sample for the sequential test. We consider a cooperative *grouped-compressed-data SPRT* (GCD-SPRT), which differs from the conventional SPRT in four perspectives: 1) Instead of taking N Nyquist samples, in each T_s, an SU randomly takes a number of sub-Nyquist samples $M << N$; 2) These samples are grouped into a "super-sample" to avoid the complexity of processing each and more importantly to reduce the effect of short-term channel randomness; 3) An SU applies sequential detection to a set of super-grouped samples from different time periods, taking advantage of the temporal redundancy and diversity to make for more effective detection decisions; 4) An SU receiving weak signals could request cooperation from its neighbors to fuse their data along with its own, further exploring the spatial diversity to make faster detection decisions. Cooperative GCD-SPRT can be performed at an SU as follows:

Step 1: Calculate the power $z(\mathbf{y})$ from M sub-Nyquist samples.

If there is any PU signal within the wideband of interest, the sub-sample vector will be expressed as in Eq. (1). After a sensing block T_s, the normalized power of M sub-Nyquist samples contained within is

$$z(\mathbf{y}) = \frac{\sum_{i=1}^{M} y_i^2}{T_s} = \frac{f_{sub}}{M} \sum_{i=1}^{M} y_i^2, \tag{4}$$

where y_i denotes an individual sample within T_s, and $M = f_{sub} T_s$ power samples are gathered within a sensing block T_s to form the super sample.

In practice, the number of samples taken within a single T_s is fairly large. For $T_s = 1$ ms and a $0 \sim 500$ MHz wideband, the Nyquist sample number is $N = 10^6$; and even if we perform sub-sampling with one tenth of the Nyquist sampling rate, we would still have 10^5 sub-Nyquist samples. With the law of large numbers ($M \gg 10$) and central limit theorem, we have the average signal within T_s approximating Gaussian regardless of the original distribution of the PU signal, that is, $z(\mathbf{y}) \overset{i.i.d.}{\sim}$

$$\begin{cases} H_0 : \mathcal{N}(f_{sub} P_n, \frac{(f_{sub} P_n)^2}{M}), \\ H_1 : \mathcal{N}(f_{sub} P_n (1 + SNR), \frac{(f_{sub} P_n)^2 (1+SNR)^2)}{M}), \end{cases} \tag{5}$$

which can be similarly derived from the results in [17]. Here, SNR is defined as the ratio between the nominal signal power P and local noise floor $\sigma^2 = P_n W$, where P_n is the noise power spectral density (PSD) and W is the bandwidth.

Step 2: Derive the test statistic $T(z(\mathbf{y}))$ for each group.

The log-likelihood ratio (LLR) of the power sample is calculated as

$$T(z(\mathbf{y})) = \ln \frac{f_1(z(\mathbf{y}))}{f_0(z(\mathbf{y}))}, \tag{6}$$

where $f_0(\cdot)$ and $f_1(\cdot)$ are the probability density functions (PDFs) under H_0 and H_1, respectively, as indicated in Eq. (5).

Step 3: Accumulate the test statistics $T(z)$ across groups to obtain the aggregate test statistic $\mathcal{T}$.

As we accumulate $T(z_k)$ ($k = 1, 2, ...$) sequentially, the aggregate test statistic up to the s-th group is

$$\mathcal{T}_s = \sum_{k=1}^{s} T(z_k) = \sum_{k=1}^{s} \ln \frac{f_1(z_k)}{f_0(z_k)}. \tag{7}$$

Step 4: On-demand cooperation with other users.

If a user cannot make timely detection decisions, it can request its neighbors to collaborate. In response, an SU q can share its own aggregated test statistic $\mathcal{T}_{s_q}^q$. Assume the user receives responses from $(Q-1)$ cooperating users, it can form the cumulative cooperative test statistic as

$$\mathcal{T}_s' = \mathcal{T}_s + \sum_{q=1}^{Q-1} \mathcal{T}_{s_q}^q. \tag{8}$$

Step 5: Make a detection decision.

The cumulative cooperative test statistic in Eq. (8) is compared against two constant thresholds A and B. With the requirement of false alarm and missed detection probabilities P_{FA} and P_{MD}, the two decision thresholds are chosen in Wald's SPRT as

$$A = \ln \frac{P_{MD}}{1 - P_{FA}}, \text{ and } B = \ln \frac{1 - P_{MD}}{P_{FA}}. \tag{9}$$

The decision rule for the SU is designed as

- if $\mathcal{T}_s' > B$, it decides that the PU has reclaimed the channel;
- if $\mathcal{T}_s' < A$, it decides that the channel is still available;
- otherwise, it goes to **Step 1** to continue sampling another group of power data, cooperating with other users, and updating $\mathcal{T}'_{s+1}$ using Eq. (8).

The *stopping time* S for an SU is defined as the minimum number of groups of LLR statistics (of the user itself) needed until one of the two decision thresholds is first crossed:

$$S = \min\{s: \text{ either } \mathcal{T}'_s < A \text{ or } \mathcal{T}'_s > B\}. \tag{10}$$

If S is small, the SU can make the detection decision faster. This helps the SU evacuate the channel in a timely manner upon the return of PU, or spend more time for its own data transmission upon detecting the channel as idle.

B. Analysis on Stopping Time

In this subsection, we provide some analytical results for sequential detection, including the expected values of the test statistics, the average stopping time, and the average sensing overhead. The proofs in this subsection are omitted due to space constraint.

Proposition 1. *Each of the i.i.d. test statistics $T(z)$ has the expected values*

$$m_0 \triangleq \mathbb{E}[T(z)|H_0] = -\frac{M-1}{2}\frac{SNR^2}{(1+SNR)^2} + \frac{SNR}{(1+SNR)^2} - \ln(1+SNR), \tag{11}$$

and

$$m_1 \triangleq \mathbb{E}[T(z)|H_1] = \frac{M+1}{2}SNR^2 + SNR - \ln(1+SNR), \tag{12}$$

under H_0 and H_1, respectively.

The above m_0 and m_1 are the average increments at each step of the sequential test. For a given M, both values depend solely on SNR. With low channel SNRs, $SNR \to 0^+$, we have

$$m_0 \approx -\frac{M}{2}SNR^2, \text{ and } m_1 \approx \frac{M}{2}SNR^2. \tag{13}$$

That is, the absolute values of the average increments under H_0 and H_1 are roughly the same when the channel SNR is low; in other words, the underlying sequential test runs at the same rate under both hypotheses.

In general, the exact distribution of the test statistic is difficult to derive; however, when the SNR is low, the distributions under H_0 and H_1 can be approximated as Gaussian, as shown below.

Proposition 2. *Under low-SNR conditions, we have*

$$T(z) \overset{i.i.d.}{\sim} \begin{cases} H_0 : \mathcal{N}(m_0, 2m_1), \\ H_1 : \mathcal{N}(m_1, 2m_1), \end{cases} \tag{14}$$

in which m_0 and m_1 are given in Eq. (13).

Next we consider the average stopping time – the average number of sample groups that need to be collected in order to reach either decision threshold.

Proposition 3. *Regardless of the SNR value, the average run lengths S for the SU to make a decision on the channel state under H_0 and H_1 are*

$$\mathbb{E}[S|H_0] = \frac{P_{FA}B + (1-P_{FA})A}{m_0} \tag{15}$$

$$\text{and } \mathbb{E}[S|H_1] = \frac{(1-P_{MD})B + P_{MD}A}{m_1} \tag{16}$$

respectively. From Eqs. (9), (15), and (16), when $P_{FA} = P_{MD}$, we have $A + B = 0$ and $\mathbb{E}[S|H_0] = \mathbb{E}[S|H_1]$. That is, the sequential test has a symmetric structure and it takes an equal number of steps on average to reach either decision boundary. If more strict requirement is imposed on P_{MD} to ensure the interference minimal to the PUs, i.e., $P_{MD} \ll P_{FA}$, we would have $|A| >> |B| \approx -\ln P_{FA}$. In this case, even with nearly identical increments $|m_0| = |m_1|$ when the channel SNR is very low, the upper threshold takes much less time to be crossed. Thus, when the PU is indeed present, the SU is expected to make the correct decision quickly.

C. Quick Detection of Spectrum State Changes and Scheduling of Detection

It is important to detect the "change point" quickly where the wideband state shifts from H_0 to H_1 due to PU reappearance or vice versa. A sensing decision can be made once in each CDT window. After a channel is detected to be idle, an SU can dedicate to transmission as shown in Figure 4(a); similar structure without compressed sensing is given in [21]. However, if the PU reappears, the channel will not be sensed until the next CDT window, which may make the evacuation delay of the SU exceed the CDT time, the maximum delay allowed for an SU to evacuate the channel.

Instead, we consider using backward GCD-SPRT along with a moving CDT window (Figure 4(b)), where GCD-SPRT can run *backward*, starting from the latest group of data. This helps reduce the impact of the older sensing data to detect the possible status change more quickly. In order to further speed up the change point detection, we propose an in-depth sensing method in which a CR adjusts its sensing frequency to ensure more rapid and precise detection after suspecting the possible H_0-to-H_1 transition, as in Figure 4(c).

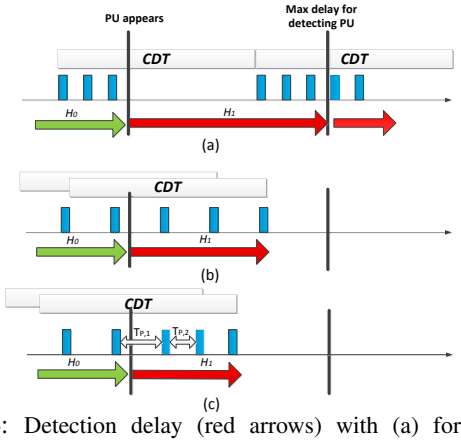

Figure 4: Detection delay (red arrows) with (a) forward, non-overlapping GCD-SPRT; (b) backward, overlapping GCD-SPRT; and (c) backward, overlapping GCD-SPRT with short-term T_p adjustment

It is critical to determine when an *in-depth sensing* should be triggered. We set the following criterion:

$$\mathcal{T}_c = \max\{\bar{T}_{new} - \bar{T}_{old}\} \geq \delta(n_{new}\frac{B}{n} - n_{old}\frac{A}{n}),$$

in which $\mathcal{T}_c$ is the test statistic that will trigger in-depth sensing; $\bar{T}_{new}$ and $\bar{T}_{old}$ are respectively the sums of the newer and older test statistics in the CDT-window, n_{new} and n_{old} are the numbers of test statistics classified as newer and older, and $n = n_{new} + n_{old}$; B and A are the thresholds in Eq. (9), and δ is the parameter that controls the sensitivity of SU to the shift. With a smaller δ value, SU is more sensitive to the changes in the observed data.

For the given set of test statistics in the CDT-window, the SU starts with the most recent test statistic (with the remaining sensing blocks in the window as "old") and obtains the difference; then the new set contains one more recent test statistic which is removed from the old set, so the numbers of newer test statistics and older ones are increased and decreased by one respectively. This continues until the data from a CDT-window have all been checked. If Eq. (17) is still not met, then GCD-SPRT-based sequential detection is pursued with T_p unchanged; otherwise, T_p will be changed and an in-depth sensing is performed to speed up the decision process. Choices of T_p will be discussed in the simulations.

A summary of our proposed wideband detection scheme is given in Algorithm 1.

V. Cooperative Wideband Compressed Sensing

After detecting the existence of PU activities in a wideband, it is necessary to determine which sub-channels are actually occupied so the remaining spectrum can be used by SUs for their own transmissions. We explore the use of compressive sensing to reconstruct the spectrum usage map from the sub-sampled data. This recovery can be done by individual users independently; however, if a user receives weak signals, the accuracy of spectrum reconstruction could be very low, and a user may need to sense the spectrum over a much longer duration with many groups of samples. To alleviate the problem, we first propose intra-user compressed sensing where a user fuses its samples in the time domain, taking advantage of the temporal diversity, to improve the reconstruction performance. If such temporal fusion is not enough, spatial sparsity from users in a neighborhood will be utilized in the inter-user cooperation triggered on demand. We consider two major strategies for user collaboration: 1) Cooperative recovery of the spectrum usage maps by utilizing joint sparsity of the samples from neighboring users to significantly reduce both the computational overhead for multi-user CS reconstruction and the number of samples to send to the requesting user, and 2) Fusion of spectrum maps, where neighbors send only their spectrum maps to the requesting user, leading to a lower signaling overhead.

A. Intra-User Compressed Sensing: Wideband Spectrum Usage Detection

To detect which sub-channels are currently occupied, we can simply use the samples taken from the most recent period. However, if the SNR is low, the signal occupancy map recovered may not be accurate enough. Given a set of samples collected from multiple time periods in sequential detection, a user can first fuse its samples over time. The question is, how many temporal samples should we use and how to fuse them?

If samples are taken across the change point, the time instant that the spectrum activities change, the fusion of samples may compromise the sensing performance. To fuse the temporal samples over a duration of time, we select the starting time based on the results from sequential detection. In Eq. (7), detection is only made when a sequence of $T(z_k)$ possess the same sign (either positive or negative) and their cumulative values exceed a threshold. Consider the beginning instant of this sequence to be k'; a user will fuse the samples from k' until the most recent instant k''.

As the user senses the same wideband spectrum over time, the basis $\mathbf{\Psi}$ for a signal to project to remains the same. If an SU adopts the same measurement matrix $\mathbf{\Phi}$ before a local sequential detection decision is made, we can take the average $\overline{\mathbf{y}} \in \mathbb{R}^{M\times 1}$ of the compressed readings from the time periods between k' and k'':

$$\overline{\mathbf{y}} = \mathbf{\Phi}(\overline{\mathbf{d}} + \overline{\mathbf{n}'}) = \mathbf{\Phi}\overline{\mathbf{d}} + \mathbf{n} = \mathbf{\Phi}\mathbf{\Psi}\overline{\mathbf{x}} + \overline{\mathbf{n}} = \mathbf{A}\overline{\mathbf{x}} + \overline{\mathbf{n}},$$

where we have the sparse vector in Fourier spectrum domain $\overline{\mathbf{x}} \in \mathbb{R}^{N\times 1}$, additive noise in the wideband $\overline{\mathbf{n}'}$, the sampled noise $\overline{\mathbf{n}} \in \mathbb{R}^{M\times 1}$, and the sensing matrix $\mathbf{A} \in \mathbb{R}^{M\times N}$. Each user can individually recover its $\overline{\mathbf{x}}$ by solving the optimization problem in Eq. (2).

In what follows, we investigate the benefit of exploiting cooperative compressive sensing. For simplicity, we will now drop the bar symbol and denote the averages for the q-th secondary user as $\mathbf{y}_q, \mathbf{x}_q$, etc., $q \in \{1, 2, ..., Q\}$, where Q is the number of SUs.

B. Inter-User Cooperation Case 1: Joint Reconstruction of Wideband Maps

Each user can independently perform wideband spectrum sensing with the number of CS samples sufficient to reconstruct the spectrum map. In the case of multiple users coexisting in a neighborhood, a user experiencing severe channel conditions or low SNRs can initiate on-demand cooperation from other users. In a dedicated control channel, every SU can share its average signal samples (obtained from intra-user cooperation in Section V-A) with nearby users within its transmission range and then perform joint reconstruction of the wideband signals. The joint reconstruction can be performed either by each cooperating user in a distributed manner (users share data with one another) or by a selected fusion node (e.g. the user that calls the cooperation) in a centralized manner. Deciding which fusion nodes to perform the joint reconstruction is beyond the scope of this work.

With data from Q users, a straightforward way to implement cooperation is to concatenate samples from all the users and process them together using a super CS matrix. However, this can easily introduce a high computational overhead. As samples from neighboring SUs may be spatially correlated, the redundancy wihtin would not effectively contribute to the CS recovery process. We utilize the Joint Sparsity Model 1 (JSM-1) [5] to significantly reduce the number of measurements and reconstruction overhead.

The spatial correlation manifests itself where the readings at nearby users may have common factors, generally introduced by PU group activities. Besides, the readings at each user also exhibit localized characteristics due to factors such as spatial location and local noise. The actual PU signal (before sub-Nyquist sampling) received at a secondary user q, $q \in \{1, 2, ..., Q\}$, can be expressed as:

$$\mathbf{d}_q = \mathbf{s}_c + \mathbf{s}_q, q \in \{1, 2, ..., Q\}, \tag{17}$$

where

$$\mathbf{s}_c = \mathbf{\Psi}\mathbf{x}_c, \|\mathbf{x}_c\|_0 = K_c, \mathbf{s}_q = \mathbf{\Psi}\mathbf{x}_q, \|\mathbf{x}_q\|_0 = K_q, \tag{18}$$

where $\mathbf{s}_c$ is the *sparse-common* component that is common to $\mathbf{d}_q$ and has sparsity K_c in the basis $\mathbf{\Psi}$. $\mathbf{s}_q$ is the *sparse-innovations* (unique portions) of the $\mathbf{d}_q$ and each has sparsity K_q in the same basis.

We can see the benefit of exploiting the joint sparsity in a simple case of $Q = 2$ users, when a node collaborates with its most nearby node. If CS is directly employed, we may need the number of measurements in the order of $c(K_c + K_1)$ to reconstruct $\mathbf{d}_1$ and $c(K_c+K_2)$ to reconstruct $\mathbf{d}_2$, respectively. To recover the two signals together, we only need $c(K_c+K_1+K_2)$ measurements.

For cooperative recovery of signals from Q users, let $\Lambda := \{1, 2, \ldots, Q\}$ denote the set of indices for the Q signals in the ensemble. Denote the *signal* in the ensemble by $\mathbf{d}_q \in \mathbb{R}^{\mathbb{N}}$, which is sparse in basis $\mathbf{\Psi}$, with $q \in \Lambda$. To compactly represent the signal and measurement ensembles, we denote $\widetilde{M} = \sum_{q\in\Lambda} M_q$ and define $\mathbf{X}$, $\mathbf{D}$, $\mathbf{Y}$, and $\widetilde{\mathbf{\Phi}}$, and $\widetilde{\mathbf{\Psi}}$ as

$$\mathbf{X} = [\mathbf{x}_c\ \mathbf{x}_1\ ...\ \mathbf{x}_Q]^T,\ \mathbf{Y} = [\mathbf{y}_1\ ...\ \mathbf{y}_Q]^T,\ \mathbf{D} = [\mathbf{d}_1\ ...\ \mathbf{d}_Q]^T, \tag{19}$$

and

$$\widetilde{\mathbf{\Phi}} = \begin{bmatrix} \mathbf{\Phi}_1 & \mathbf{0} & \ldots & \mathbf{0} \\ \mathbf{0} & \mathbf{\Phi}_2 & \ldots & \mathbf{0} \\ \vdots & \vdots & \ddots & \vdots \\ \mathbf{0} & \mathbf{0} & \ldots & \mathbf{\Phi}_Q \end{bmatrix}, \tag{20}$$

$$\widetilde{\mathbf{\Psi}} = \begin{bmatrix} \mathbf{\Psi} & \mathbf{\Psi} & \mathbf{0} & \ldots & \mathbf{0} \\ \mathbf{\Psi} & \mathbf{0} & \mathbf{\Psi} & \ldots & \mathbf{0} \\ \vdots & \vdots & \vdots & \ddots & \vdots \\ \mathbf{\Psi} & \mathbf{0} & \mathbf{0} & \ldots & \mathbf{\Psi} \end{bmatrix}. \tag{21}$$

Using the structured $\widetilde{\mathbf{\Psi}}$, we can represent $\mathbf{D}$ sparsely using vector $\mathbf{X}$, which contains $K_c + \sum_{q=1}^{Q} K_q$ non-zero elements, to obtain $\mathbf{D} = \widetilde{\mathbf{\Psi}}\mathbf{X}$. We then have $\mathbf{Y} = \widetilde{\mathbf{\Phi}}\widetilde{\mathbf{\Psi}}\mathbf{X} = \widetilde{\mathbf{A}}\mathbf{X}$. With sufficient measurements, we can recover the vector $\mathbf{X}$, and thus $\mathbf{D}$ (all $\mathbf{d}_q$) and wideband status ($\mathbf{x}_c + \mathbf{x}_q$), by solving the following problem:

$$\min \quad \|\mathbf{X}\|_{\ell_1} \tag{22a}$$

$$\text{s.t. } \mathbf{Y} = \widetilde{\mathbf{\Psi}}\widetilde{\mathbf{\Phi}}\mathbf{X} \tag{22b}$$

with CS construction algorithms such as the one in [7]. After receiving compressed readings $\mathbf{y}_q$ from all users, a fusion node can form new matrices as in Eqs. (19)-(21) and solve the problem as in Eq. (22). Then the estimated wideband status map for each user is expressed as $\mathbf{x}_c + \mathbf{x}_q$.

C. Inter-User Cooperation Case 2: Fusion of Wideband Spectrum Maps

The cooperative compressive sensing in case 1 requires the exchange of data samples among users, and the overhead could be high if a large number of samples are exchanged. As an alternative, we also provide a set of spectrum-map-based cooperative schemes. A user in need of cooperation can choose to fuse the spectrum maps from nearby users, either for achieving a consensus of the sub-band usage status or for facilitating a user suffering from severe fading to learn about the spectrum occupancy condition.

1) Fusion schemes: The maps from multiple users may be fused with different schemes. We consider the following four strategies:

(a) **Soft Fusion.** Power spectrum usage maps recovered by all users are averaged to obtain a new map, and each sub-band value is compared with an energy threshold to determine which sub-bands are occupied.

Let P_q^j be the estimated power at user q ($q = 1, 2, ..., Q$) for sub-band j ($j = 1, 2, ..., J$). Then for each sub-band j, the fused power spectrum value P^j is expressed as

$$P^j = \frac{\sum_{q=1}^{Q} P_q^j}{Q}. \tag{23}$$

(b) **Hard Fusion.** The spectrum energy map from each user is applied to determine which sub-bands are occupied individually, and the resulting binary spectrum maps (where the occupied sub-bands marked as "1" and the idle ones marked as "0") are merged by the OR rule (alternatively, AND rule, majority rule, etc.).

(c) **Wideband SNR Weighted Fusion.** Rather than fusing the maps from all users equally, the ones with higher SNRs would contribute more to the accurate spectrum occupancy detection. In wideband SNR weighted fusion, we take into account the effects of users' wideband SNRs by weighting the spectrum signal of a node with the SNR of its sensed wideband signal and combine the weighted information from all the users to obtain the fusion results.

Let SNR_q be the wideband SNR for user q ($q = 1, 2, ..., Q$) and P_q^j be the estimated power at user q for sub-band j ($j = 1, 2, ..., J$), then for each sub-band j, the fused power spectrum value P_j is weighted in the following form:

$$P^j = \sum_{q=1}^{Q} \frac{SNR_q}{\sum_{q=1}^{Q} SNR_q} P_q^j. \tag{24}$$

(d) **Sub-carrier SNR Weighted Fusion.** Each sub-carrier may experience different channel conditions and has different SNRs. In sub-carrier or sub-band SNR weighted fusion, we consider the signal strength over each sub-channel in the wideband. More specifically, this scheme obtains the status of each sub-band by weighting the sub-carriers by their individual SNRs, and the weighted sums of the sub-carriers are further applied to determine the spectrum activity.

Let SNR_q^j and P_q^j be the SNR and estimated power at user q ($q = 1, 2, ..., Q$) for sub-band j ($j = 1, 2, ..., J$), respectively, then for each sub-band j, the fused power spectrum value P^j

is weighted in the following form:

$$P^j = \sum_{q=1}^{Q} \frac{SNR_q^j}{\sum_{q=1}^{Q} SNR_q^j} P_q^j. \quad (25)$$

Comparing the two weighted fusion schemes, the sub-carrier SNR weighted scheme may allow for more efficient fusion. However, transmitting SNRs of all sub-carriers would introduce higher signaling overhead. We will evaluate the trade-off between detection accuracy and the signaling overhead in our performance studies.

2) Additional sampling and fusion delay: In previous discussions, the signal samples from the time of change detection to the decision-making are used to reconstruct the wideband spectrum map and find the detailed activities of PUs. As our spectrum monitoring is long-term, new measurement samples will no longer be used for this round of sensing process but only for the detection of a possible PU activity change. Although enough samples have been collected to determine whether there exists a PU activity change in a wideband, they may not be warranted for accurate reconstruction of the spectrum map to identify detailed sub-channel activities. We would like to study whether additional periods of sampling after the decision making on wideband activity can possibly further improve the accuracy in forming the spectrum map.

The additional sampling is done in a similar way as in the sequential detection process, but with a different stopping rule. The length of the sensing period (T_p) will be reset to the default value. In each additional sensing period, the user will sample the wideband with the default sensing time T_s, reconstruct its individual spectrum map, and perform the map fusion with the information from cooperative users. Its fused map is calculated by a fusion scheme introduced in Section V-C1. The user will stop gathering additional samples after the convergence stopping rule is met: the difference of fused maps between the current sensing period and the previous period falls below a threshold δ_f.

Instead of performing the map fusion only once immediately after the detection decision, additional periods of sampling will bring in further fusion delay and signaling overhead. We will study the tradeoffs in our performance studies in Section VI.

D. Anomaly Detection and Data Recovery

Abnormal readings in gathered wideband samples can significantly degrade the detection and sensing performances. In the case of map fusion discussed in Section V-C, instead of directly utilizing all the samples to recover the map, we propose that each node perform anomaly detection first. Once anomalies are detected and localized, a user can rule out the impacts of abnormal readings and recover the spectrum map more accurately, thus a "better" map can be supplied to the fusion process. Similar techniques can also be used in the joint reconstruction case in Section V-B.

The anomalies usually occur in the form of spikes of burst data, which indicates the aforementioned abnormal readings hiding in the measured data are usually sparse. This serves as a foundation for us to exploit CS to identify these anomalies and reduce their effects on sensing performance. From the theory of overcomplete representation basis [19], we exploit combinational sparsity to simultaneously capture both the signals of interest and the anomalies, where sensed data $\mathbf{d}$ can be decomposed into regular data $\mathbf{d_r}$ and the abnormal activity $\mathbf{d_a}$. Mathematically, the received data at a node can be expressed as

$$\mathbf{d} = \mathbf{d_r} + \mathbf{d_a} = \mathbf{\Psi x_r} + \mathbf{d_a} = [\mathbf{\Psi\ I}][\mathbf{x_r} \quad \mathbf{d_a}]^T = \mathbf{\Psi' x}, \quad (26)$$

where

$$\mathbf{\Psi'} = [\mathbf{\Psi\ I}] \text{ and } \mathbf{x} = [\mathbf{x_r} \quad \mathbf{d_a}]^T. \quad (27)$$

After sub-sampling,

$$\mathbf{y} = \mathbf{\Phi}(\mathbf{d} + \mathbf{n'}) = \mathbf{\Phi d} + \mathbf{n} = \mathbf{\Phi \Psi' x} + \mathbf{n} = \mathbf{A' x} + \mathbf{n}. \quad (28)$$

According to the CS theory, one is able to recover the sparse vector $\mathbf{x}$, and thus the regular portion $\mathbf{d_r}$ and anomalous portion $\mathbf{d_a}$ of the data from the contaminated measurement $\mathbf{d}$. If a large non-zero value is detected in $\mathbf{d_a}$, then there exists an abnormal reading in the measured data.

The proposed anomaly detection scheme is summarized in Algorithm 3, which can be performed either (a) by each node individually or (b) at the fusion node. In the following simulations, we will study the benefits of anomaly detection in individual user cases.

Algorithm 1 Wideband detection for each SU

Require:
(1) Initialization (details in Section IV). (2) Generate the pseudo-random sub-Nyquist measurement matrix $\mathbf{\Phi}$ as described in Section III-B.
Ensure:
1: **Sub-sampling**
For each sensing block T_s, sub-sample with $\mathbf{\Phi}$, collect sub-Nyquist samples $\mathbf{y}$ expressed in Eq. (1).
2: **Detection of Potential Change**
Calculate test statistics described in GCD-SPRT (Section IV-A) and perform change detection (Section IV-C).
If Eq. (17) is not met, then T_p remains unchanged. Go to **Backward GCD-SPRT**.
Otherwise, change is suspected and in-depth sensing is triggered. Go to **In-depth Sensing**.
3: **Backward GCD-SPRT**
Perform Cooperative Backward GCD-SPRT described in Section IV.
Make decision of wideband detection (PU is present/absent). End of algorithm.
If decision cannot be made, slide the CDT-window forward by T_p from the current one, iterate until decision can be made.
4: **In-depth Sensing**
New sensing period T_p is determined for the periodic sensing model and CDT-window slides forward by new T_p. Go to **Backward GCD-SPRT**.

Algorithm 2 Cooperative wideband sensing at fusion node

Require:
Initialization.
Ensure:
1: **Information Exchange. Fusion node obtains other users' data.**
Case 1: temporal averaged samples (Section V-B);
Case 2: spectrum maps (Section V-C).
2: **Collaboration**
Case 1: joint reconstruction of spectrum map from users' samples;
Case 2: fusion of the users' spectrum maps.

VI. Simulations and Results

In this section, we conduct extensive simulation studies to demonstrate the performance of our design compared to peer schemes.

Algorithm 3 Anomaly detection and regular data retrieval

Require:
(1) Initialization. (2) Measurement $\mathbf{y}$.
Ensure:
1: **Anomaly detecting compressed sensing**

$$\min\|\mathbf{x}\|_{\ell_1}, \quad \text{s.t. } \left\|\mathbf{A}'\mathbf{x}-\mathbf{y}\right\|_{\ell_2} \leq \epsilon, \mathbf{A}' = \mathbf{\Phi}\,\mathbf{\Psi}' = \mathbf{\Phi}\begin{bmatrix}\mathbf{\Psi} & \mathbf{I}\end{bmatrix} \quad (29)$$

where the parameter ϵ is the bound of the error.
2: **Regular data and anomaly data separation**
From $\mathbf{x}$ and Eqs. (26) and (27), obtain regular data $\mathbf{d_r}$ and anomaly data $\mathbf{d_a}$.
3: **Anomaly Detection**
As discussed in Section V-D, if a large non-zero value is detected in $\mathbf{d_a}$, then there exists an abnormal reading in the measured data. The more non-zero elements in $\mathbf{d_a}$, the more likely the user is under significant influence of anomalies and prone to malfunction.
4: **Further processing with regular data**
The reconstructed regular data $\mathbf{d_r}$, instead of anomaly contaminated data $\mathbf{d}$, is further exploited by each user to perform wideband sensing described.

Table I: Default parameters

Parameter	Description
sensing block duration	$T_s = 20\mu$s
channel detection time	$CDT = 400$ms
required error probabilities	$P_{FA} = P_{MD} = 0.1$
sub-Nyquist sampling rate	$f_{sub} = 0.25$ GHz
# compressed samples in T_s	$M = f_{sub}T_s = 5000$
Nyquist number	$N = f_{nyq}T_s = 20,000$

A. Simulation Settings

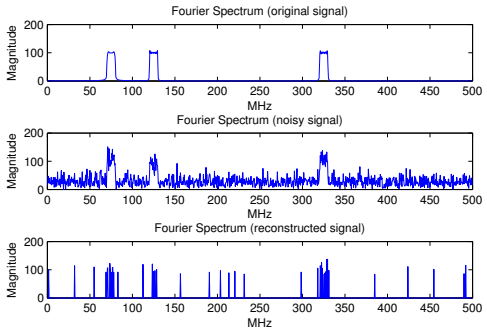

Figure 5: Example of wideband sensing under $SNR = -5dB$

1) System Setup: We consider a wideband of 500 MHz, which can be virtually divided into 50 sub-bands, each occupying 10 MHz. The Nyquist sampling rate is $f_{nyq} = 1$ GHz. A PU group signal is a wideband signal that spreads over the wideband but may only occupy a small portion of it; i.e., the number of occupied sub-bands is much smaller than the total number of sub-bands monitored. The noise is assumed to be circular complex AWGN, i.e., $\mathbf{n} \sim \mathcal{N}(0, \eta^2)$. The SNR values will be given in specific tests.

Default parameter settings are shown in Table I. An example of the wideband signal spectrum, noise spectrum, and recovered spectrum using CS is presented in Figure 5, where the SNR is -5 dB. The wideband signal shown in this example has three occupied sub-bands that have center frequencies of 75, 125, and 225 MHz respectively and each sub-band has a bandwidth of 10 MHz. We also set the MAC frame size $FS = 200\mu$s. For the sensing period T_p, we adopt the settings similar to those in [17].

Throughout simulations, we use ℓ_1-magic as the basic reconstruction algorithm [7]. Some other modified reconstruction algorithms can also be used, such as those greedy algorithms proposed in [33].

2) Schemes and Performance metrics: The peer schemes we compare with in our simulations are summarized in Table II. The option "reference" is the scheme with proposed sequential detection but with Nyquist sampling (without using CS). We use "reference" as a benchmark to evaluate the performance of using sub-sampling with our proposed scheme. The scheme "conv1" uses conventional non-overlapping forward SPRT without CS, whereas "conv2" reconstructs signals every T_p in order to use recovered signals to perform sequential detection and identify the actual spectrum channel occupancy. In the collaborative sensing case, "conv2" concatenates the signals from multiple users to form a super matrix for further reconstruction. Table II also lists the default SNR for each scheme (if not otherwise stated): for group 1 schemes, -18.8 dB; for group 2, -5 dB. In group 3, each fusion scheme has been introduced in Section V-C1.

Table II: Peer schemes comparison

Group 1: default *SNR*$= -18.8$dB
"proposed": $\delta = 2$, $T_p^{new} \leftarrow 2FS$
"proposed-snr1" : proposed with *SNR*$= -22.8$dB
"proposed-snr2" : proposed with *SNR*$= -20.8$dB
"conv1" : non-overlapping forward SPRT w/o CS, see Fig. 4(a) and [21]
"reference" : proposed sequential w/o CS, i.e., with Nyquist sampling

Group 2: default *SNR*$= -5$dB
"proposed-joint": proposed joint recovery among SUs
"proposed-joint1" : proposed with *SNR*$= -15$dB
"proposed-joint2" : proposed with *SNR*$= -10$dB
"conv2" : with CS, reconstruct signals each T_p for sequential detection
"peer2" : with CS, concatenated signal reconstruction, see [31]

Group 3: Map Fusion Schemes, see Sec. V-C
"SF": Soft Fusion
"HF" : Hard Fusion
"W-SNR-WF" : Wideband SNR Weighted Fusion
"S-SNR-WF" : Sub-band SNR Weighted Fusion
"JR" : proposed joint recovery

Some performance metrics used in our studies are defined as follows:

- Detection delay: The time it takes for a secondary user to determine whether there exist PUs in the wideband.
- Detection accuracy: The probability of successfully detecting if there exist PUs in the wideband, i.e., detecting with neither false alarm nor missed detection.
- Wideband sensing accuracy: The percentage of the sub-bands in the overall wideband that are correctly detected regarding their activity status. This accuracy depends on the channel measurement rate, defined as the ratio of sub-Nyquist rate to the Nyquist rate.
- reconstruction computational overhead: The actual running time used to complete the CS reconstruction.
- number of CS reconstructions: The number of CS reconstructions performed based on the compressed (subset of) samples. Each CS reconstruction occurs in one or several sensing periods, depending on the scheme.
- Fusion delay: Delay introduced by taking additional samples for more accurate fusion as introduced in Section V-C2.
- Total delay: Sum of detection delay and fusion delay.
- Signaling overhead: The total amount of information transmitted from the time when the PU detection decision

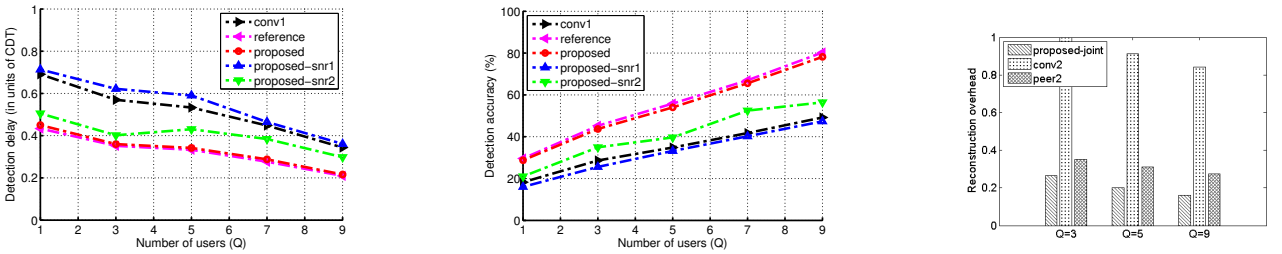

(a) Detection delay (b) Detection accuracy (c) CS reconstruction overhead

Figure 6: Effects of number of users

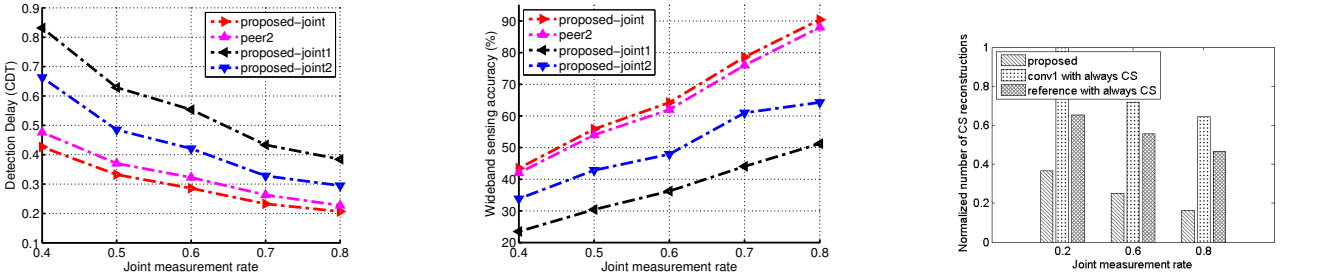

(a) Detection delay (b) Wideband sensing accuracy (c) # CS reconstructions before decision

Figure 7: Effects of joint measurement rate

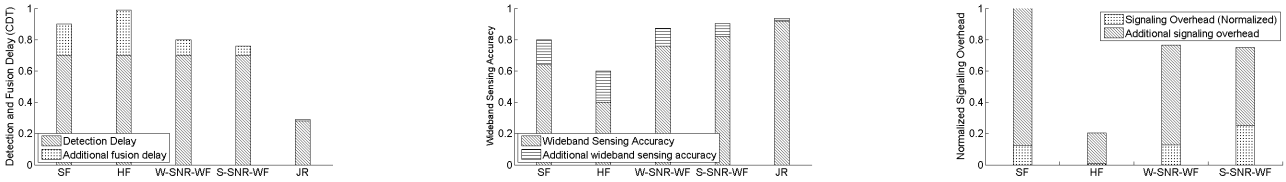

(a) Detection delay and fusion delay (b) Wideband sensing accuracy (c) Signaling overhead

Figure 8: Comparisons of fusion schemes

is made until the completion of the map fusion process, i.e., the cost of information exchange during the fusion process.

B. Performance and Analysis

1) Impacts of number of users: We vary the number of cooperating users in Figure 6(a), and as expected, the detection delay for all schemes reduces as the number of users increases. This clearly indicates the benefit of our cooperative sensing. The delay values of "proposed" and "reference" are very similar, which indicates that CS-based sequential detection is effective and can achieve comparable performance even with samples much fewer than required by Nyquist sampling. With our proposed scheme under lower SNRs in "proposed-snr1" and "proposed-snr2", the detection delay is larger as expected, which indicates that channel conditions have a significant impact on the detection delay. A user in extreme environmental situations may not be able to make the detection decision by itself and thus the sensing cooperation is needed to alleviate this problem. In addition, compared with "conv1", our proposed scheduling of GCD-SPRT scheme can make a decision with a much shorter delay, thus accelerating the detection process and avoiding transmission conflictions with primary users. The delay reduction is up to a third when compared to "conv1".

In Figure 6(b), although only a quarter of the samples are used, our proposed scheduled GCD-SPRT scheme can achieve the detection accuracy similar to that using the Nyquist-sampling ("reference"). Compared to "conv1", GCD-SPRT achieves up to 60% higher accuracy, even though "conv1" uses more samples in each period. This shows the benefit of exploiting compressed sensing and our backward sequential sensing. We also see that when the number of users (Q) increases, the detection accuracy improves more rapidly, which again demonstrates the advantage of cooperation among SUs.

In Figure 6(c), the computational overhead for CS reconstruction is compared. For ease of presentation, we normalize this overhead by dividing it by the largest value in the figure, i.e., the scheme "conv2" with the number of users $Q = 3$. We can see that among all the schemes, our proposed joint recovery scheme results in the least overhead. Compared to "conv2", which is the sequential detection scheme with the CS reconstruction scheduled once every sensing period T_p, the overhead for CS reconstruction in our proposed scheme is about 80% lower when $Q = 9$. This is a very promising improvement considering the number of samples is often very large in wideband sensing.

2) Impacts of measurement rate: Figure 7(a) depicts the impacts of the joint measurement rate on detection delay. The delay is reduced as the measurement rate increases. The smaller the measurement rate, the fewer samples are gathered

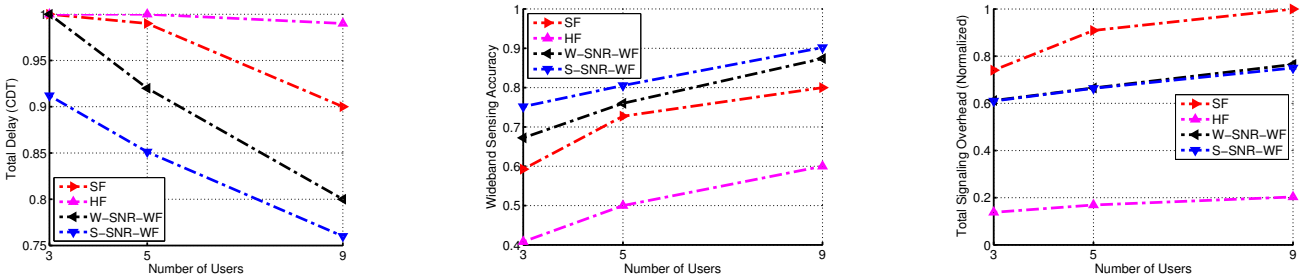

(a) Total delay (b) Total wideband sensing accuracy (c) Total signaling overhead

Figure 9: Impacts of number of users on fusion schemes with additional sampling

(a) Detection delay (b) Wideband sensing accuracy

Figure 10: Impacts of anomaly detection

in the sequential detection, hence the longer it takes to make a detection decision. At the measurement rate of 0.6, our proposed joint recovery scheme reduces the detection delay by 12% compared to "peer2", the latter of which simply puts together samples from all users for signal reconstruction.

From Figure 7(b), as the measurement rate becomes larger (i.e., more samples are taken in the sub-sampling process), the accuracy of wideband sensing increases, which agrees with the CS theory. At the same measurement rate of 0.6, our scheme outperforms "peer2", which shows the advantages of joint CS reconstruction in achieving a higher signal reconstruction accuracy. Comparing the joint scheme under different SNRs, if we draw a horizontal line corresponding to a sensing accuracy, we can see the number of measurements needed increases when the SNR is lower. With the same SNR, compared to "peer2" that uses long concatenated signal samples to perform reconstruction, the joint recovery scheme can actually reduce the measurement rate to reach the same wideband sensing accuracy. The reason is that we exploit the temporal and spatial correlations in sensing data to further reduce the measurement requirement for reconstructing every user's signal.

In Figure 7(c), the number of CS reconstructions of different schemes is compared, where the values are normalized (divided by the largest value in the figure, i.e., the scheme "conv1 always with CS" with a joint measurement rate of 0.2). Among all the schemes, our proposed scheduling of CS-based detection with joint signal recovery scheme requires the least number of CS reconstructions. When the joint measurement rate is 0.8, compared to "conv1 always with CS" which has the conventional sequential detection with CS reconstruction in every sensing period, and "reference always with CS" which uses our sequential detection scheduling but always performs CS in each sensing period, our proposed scheme reduces the number of CS reconstructions by about 75% and 65%, respectively. This overhead reduction is the joint effect of smart scheduling of sequential detection and on-demand compressed sensing.

3) Impacts of Additional Sampling: Rather than recovering the spectrum map with joint CS recovery among neighbors, to avoid the need of transmitting measurement samples, we introduce several schemes to fuse the spectrum maps constructed by individual secondary devices. In addition, additional sampling may be taken to increase the accuracy of reconstructing the spectrum map as introduced in Section V-C2. We would like to study the trade-offs brought by the additional sampling and fusion delay. For different fusion schemes, we evaluate the additional fusion delay, improved sensing accuracy, and additional signaling overhead resulting from the additional sampling. We plot the results in Figure 8.

For the Soft Fusion, Hard Fusion, Wideband SNR Weighted Fusion, and Sub-band SNR Weighted Fusion, the use of additional sampling increases the delay by 28%, 41%, 15%, and 9%, respectively and the corresponding signaling overhead by about 700%, 2500%, 500%, and 200%. The considerable increase in delay and overhead is due to the use of additional sensing periods to achieve higher wideband sensing accuracy, and the accuracy level is seen to improve by 18%, 24%, 14%, and 10%, respectively. Compared to map fusion, the delay and wideband sensing accuracy of Joint Recovery (JR) improve respectively by 4% and 2%, but its signaling overhead can become larger by two orders of magnitude (too large and therefore not plotted in Figure 8(c)) due to the need for exchanging signal samples. As an interesting trade-off observed, if a fusion scheme requires less information exchange (a) it may need additional sampling sensing periods to achieve stable convergence (see the stopping rule in

Section V-C2), thus leading to longer fusion delay and a larger signaling overhead, and (b) it may improve the wideband sensing accuracy more rapidly with the same group of additional sampling. One reason might be that if a fusion scheme has more information exchanged from the beginning, it is likely that it will benefit less from the additional sampling due to information redundancy.

4) Impacts of number of users on Fusion Schemes with Additional Sampling: We vary the number of users and study how it affects the performances of fusion schemes with additional sampling introduced in Section V-C2. Since additional sampling is exploited, we have evaluated the total delay, total wideband sensing accuracy and total signaling overhead.

The results are shown in Figure 9. As expected, when more users collaborate in sensing, the total delay (sum of detection and fusion delay) is reduced and the wideband sensing accuracy improves. The signaling overhead increases but at a smaller scale. Although more information is exchanged in each sensing period, the fusion of results from more users reduces the number of periods needed to make detection and fusion decision.

5) Impacts of Anomaly Detection: We vary the number of anomaly-affected users and the percentage of anomalies in each user's received data to assess the impacts of anomalies and the advantage of anomaly detection in reducing the detection delay and improving the wideband sensing accuracy. We investigate the case of $Q = 5$ collaborative users, where each may be affected by 5% or 10% anomalies and the number of affected users varies from 1 to 5. The results are shown in Figure 10. The average detection delay among users becomes longer as each user encounters more abnormal readings or the number of affected users increases, which indicates the significant impacts of anomalies on the detection delay. It can also be observed that (a) the wideband sensing accuracy decreases as the number of affected users increases and/or each user experiences more abnormal readings and (b) anomaly detection significantly improves the accuracy compared to direct processing of the contaminated data without detecting anomalies. When there are $Q = 5$ users and 5% anomalies per user, compared to the scheme without considering anomalies (directly using contaminated data), anomaly detection improves the wideband sensing accuracy by 27%, and with 10% anomalies per user, by 45%. The scheme with anomaly detection is less affected by the increase in anomalies. The wideband sensing accuracy with anomaly detection degrades slower when more anomalies exist in the received data, which indicates anomaly detection performs even better in the presence of more severe abnormal readings.

VII. Conclusion

To increase wireless network capacity, we have presented an integrated framework to perform wideband detection and wideband sensing efficiently. The Compressed Sensing (CS) technique is incorporated into the scheduling of sequential detection to ensure low sensing and signaling overhead and more accurate wideband detection. To better identify the sub-bands occupied by PU, we have proposed two cooperative schemes among neighboring users. To achieve more accurate wideband sensing, an anomaly detection method is also presented. Simulation results demonstrate the significant advantages of our performance in reducing the detection delay, increasing the detection accuracy, as well as reducing the CS recovery overhead and compressive measurement requirements. Our studies also show the trade-offs between the improvement of sensing performance with lower delay and higher accuracy and the overhead incurred for computation and communications.

References

[1] Ian F. Akyildiz, Brandon F. Lo, and Ravikumar Balakrishnan. Cooperative spectrum sensing in cognitive radio networks: A survey. *Phys. Commun.*, 4(1):40–62, March 2011.

[2] H. Sun and W. Y . Chiu and A. Nallanathan. Adaptive compressive spectrum sensing for wideband cognitive radios. *IEEE Communications Letters*, 16(11):1812–1815, Nov. 2012.

[3] Y. L. Polo and Y. Wang and A. Pandharipande and G. Leus. Compressive wide-band spectrum sensing. *Proc. IEEE ICASSP*, pages 2337–=2340, 2009.

[4] Sunghwan Bae and Hongseok Kim. Robust cooperative sensing with on/off signaling over imperfect reporting channels. *IEEE Transactions on Industrial Informatics*, 12(6):2196–2205, 2016.

[5] Dror Baron, Marco F Duarte, Shriram Sarvotham, Michael B Wakin, and Richard G Baraniuk. An information-theoretic approach to distributed compressed sensing. In *Proc. 45rd Conference on Communication, Control, and Computing*, 2005.

[6] E. J. Candès. Compressive sampling. *Proc. International Congress of Mathematicians*, Madrid, Spain, 2006.

[7] E. J. Candès and J. Romberg. ℓ_1 -magic: Recovery of sparse signals via convex programming. 2005.

[8] Z. M. Charbiwala, S. Chakraborty, S. Zahedi, Y. Kim, T. He, C. Bisdikian, and M. B. Srivastav. Compressive oversampling for robust data transmission in sensor networks. *Proc. IEEE INFOCOM*, 2010.

[9] Ruilong Deng, Jiming Chen, Chau Yuen, Peng Cheng, and Youxian Sun. Energy-efficient cooperative spectrum sensing by optimal scheduling in sensor-aided cognitive radio networks. *IEEE Transactions on Vehicular Technology*, 61(2):716–725, 2012.

[10] D. L. Donoho. Compressed sensing. *IEEE Transactions on Information Theory*, 52(4):1289–1306, April 2006.

[11] M. F. Duarte, S. Sarvotham, D. Baron, M. B. Wakin, and R. G. Baraniuk. Distributed compressed sensing of jointly sparse signals. In *Conference Record of the Thirty-Ninth Asilomar Conference onSignals, Systems and Computers, 2005.*, pages 1537–1541, October 2005.

[12] J. Guo, G. Zhong, D. Qu, and T. Jiang. Multi-slot spectrum sensing with backward sprt in cognitive radio networks. *Intl. Conference on Wireless Communications & Signal Processing*, Nov. 2009, 2010.

[13] S. Haykin. Cognitive radio: brain-empowered wireless communications. *IEEE JSAC*, 23(2):201–220, Feb. 2005.

[14] H. Kim and K. G. Shin. In-band spectrum sensing in cognitive radio networks: energy detection or feature detection? *Proceedings Mobicom '08*, pages 14–25, 2008.

[15] Kwok Hung Li, Kah Chan Teh, et al. Dynamic cooperative sensing–access policy for energy-harvesting cognitive radio systems. *IEEE Transactions on Vehicular Technology*, 65(12):10137–10141, 2016.

[16] Q. Liu, X. Wang, and Y. Cui. Robust and adaptive scheduling of sequential periodic sensing for cognitive radios. *IEEE JSAC, special issue on cognitive networks*, 2014.

[17] Q. Liu, X. Wang, and Y. Cui. Scheduling of sequential periodic sensing for cognitive radios. *Proc. IEEE INFOCOM*, Apr. 2013.

[18] Yi Liu, Shengli Xie, Rong Yu, Yan Zhang, and Chau Yuen. An efficient mac protocol with selective grouping and cooperative sensing in cognitive radio networks. *IEEE Transactions on Vehicular Technology*, 62(8):3928–3941, 2013.

[19] Chong Luo, Feng Wu, Jun Sun, and Chang Wen Chen. Compressive data gathering for large-scale wireless sensor networks. In *Proceedings of the 15th Annual International Conference on Mobile Computing and Networking*, MobiCom '09, pages 145–156, New York, NY, USA, 2009. ACM.

[20] Y. Ma, Y. Gao, Y. C. Liang, and S. Cui. Reliable and efficient sub-nyquist wideband spectrum sensing in cooperative cognitive radio networks. *IEEE Journal on Selected Areas in Communications*, 34(10):2750–2762, Oct 2016.
[21] A. W. Min and K. G. Shin. An optimal sensing framework based on spatial rss-profile in cognitive radio networks. *Proc. IEEE SECON '09*, Jun. 2009.
[22] D. Needell and J. Tropp. Cosamp: Iterative signal recovery from incomplete and inaccurate samples. *Applied and Computational Harmonic Analysis*, 26(3):301–321, May 2009.
[23] Z. Qin, Y. Gao, and C. G. Parini. Data-assisted low complexity compressive spectrum sensing on real-time signals under sub-nyquist rate. *IEEE Transactions on Wireless Communications*, 15(2):1174–1185, Feb 2016.
[24] Z. Qin, Y. Gao, M. D. Plumbley, and C. G. Parini. Wideband spectrum sensing on real-time signals at sub-nyquist sampling rates in single and cooperative multiple nodes. *IEEE Transactions on Signal Processing*, 64(12):3106–3117, June 2016.
[25] D. Romero, D. D. Ariananda, Z. Tian, and G. Leus. Compressive covariance sensing: Structure-based compressive sensing beyond sparsity. *IEEE Signal Processing Magazine*, 33(1):78–93, Jan 2016.
[26] Z. Tian and G. B. Giannakis. Compressed sensing for wideband cognitive radios. *Proceedings of ICASSP*, 2007.
[27] Z. Tian, Y. Tafesse, and B. M. Sadler. Cyclic feature detection withsub-nyquist sampling for wideband spectrum sensing. *IEEE J. Sel. Topics Signal Process*, 6(1):58–69, 2012.
[28] A. Wald. Sequential analysis. *John Wiley & Sons*, New York, NY, 1947.
[29] Y. Wang, Z. Tian, and C. Feng. A two-step compressed spectrum sensing scheme for wideband cognitive radios. *Proc. IEEE Globecom '10*, Miami, USA, Dec. 2010.
[30] Fanzi Zeng, Chen Li, and Zhi Tian. Distributed compressive spectrum sensing in cooperative multihop cognitive networks. *IEEE Journal of Selected Topics in Signal Processing*, 5(1):37–48, 2011.
[31] Huazi Zhang, Zhaoyang Zhang, and Yuen Chau. Distributed compressed wideband sensing in cognitive radio sensor networks. In *Computer Communications Workshops (INFOCOM WKSHPS), 2011 IEEE Conference on*, pages 13–17. IEEE, 2011.
[32] J. Zhao and X. Wang. Channel sensing order for multi-user cognitive radio networks. *IEEE Dynamic Spectrum Access Network (IEEE DySPAN 2012)*, pages 397–407, Bellevue, Washington, Oct 2012.
[33] J. Zhao and X. Wang. Compressive wireless data transmissions under channel perturbation. *IEEE International Conference on Sensing, Communications and Networking (IEEE SECON 2014)*, pages 212–220, Singapore, June 2014.
[34] J. Zhao, X. Wang, and Q. Liu. Cooperative sequential compressed spectrum sensing over wide spectrum band. *IEEE International Conference on Sensing, Communications and Networking (IEEE SECON 2015)*, pages 1–9, Seattle, June 2015.
[35] Q. Zhao and B. M. Sadler. A survey of dynamic spectrum access. *IEEE Signal Processing Magazine*, 24(3):79–89, May 2007.

Jie Zhao received the B.S. degree in telecommunications engineering from Huazhong University of Science and Technology, Wuhan, China. Currently he is a Ph.D. candidate in the Department of Electrical and Computer Engineering, the State University of New York at Stony Brook, New York, USA. His current research interests include compressed sensing, cognitive radio networks, as well as networked sensing and detection.

Qiang Liu received the Ph.D. degree in electrical and computer engineering from Stony Brook University, Stony Brook, NY, USA, in 2014. He is currently a Research Associate in the Computational Sciences and Engineering Division at Oak Ridge National Laboratory, Oak Ridge, TN, USA. His research areas include networked data and information fusion, signal/target detection and estimation, statistical signal processing, wireless sensor networks, cognitive radios, cyber-physical systems, transport protocols, high performance computing, and software defined networking. He has published over 30 peer-reviewed papers in prestigious journals and conference proceedings, and has reviewed dozens of works by others. He has been invited to present his work at various venues and has received several best paper and travel grant awards.

Xin Wang received the B.S. and M.S. degrees in telecommunications engineering and wireless communications engineering respectively from Beijing University of Posts and Telecommunications, Beijing, China, and the Ph.D. degree in electrical and computer engineering from Columbia University, New York, NY. She is currently an Associate Professor in the Department of Electrical and Computer Engineering of the State University of New York at Stony Brook, Stony Brook, NY. Before joining Stony Brook, she was a Member of Technical Staff in the area of mobile and wireless networking at Bell Labs Research, Lucent Technologies, New Jersey, and an Assistant Professor in the Department of Computer Science and Engineering of the State University of New York at Buffalo, Buffalo, NY. Her research interests include algorithm and protocol design in wireless networks and communications, mobile and distributed computing, as well as networked sensing and detection. She has served in executive committee and technical committee of numerous conferences and funding review panels, and serves as the associate editor of IEEE Transactions on Mobile Computing. Dr. Wang achieved the NSF career award in 2005, and ONR challenge award in 2010.

Shiwen Mao received the Ph.D. degree in electrical and computer engineering from Polytechnic University, Brooklyn, NY, in 2004. He is currently the Samuel Ginn Endowed Professor and the Director of the Wireless Engineering Research and Education Center with the Samuel Ginn College of Engineering, Auburn University, Auburn, AL, USA. His research interests include wireless networks and multimedia communications, such as cognitive radio, small cells, millimeter wave networks, free space optical networks, localization, and smart grid. He received the 2015 IEEE ComSoc Communication Switching and Routing Technical Committee (TC-CSR) Distinguished Service Award, the 2013 IEEE ComSoc Multimedia Communications Technical Committee (MMTC) Outstanding Leadership Award, and the NSF CAREER Award in 2010. He was a co-recipient of the IEEE GLOBECOM 2015 Best Paper Award, the IEEE WCNC 2015 Best Paper Award, the IEEE ICC 2013 Best Paper Award, and the 2004 IEEE Communications Society Leonard G. Abraham Prize in the Field of Communications Systems. He is a Distinguished Lecturer of the IEEE Vehicular Technology Society. He is on the Editorial Board of IEEE Transactions on Multimedia, IEEE Internet of Things Journal, IEEE Communications Surveys and Tutorials, and IEEE Multimedia.